

# DESIGN AND TEST OF THRESHING AND CLEANING DEVICE FOR *CYPERUS ESCULENTUS L.* COMBINE HARVESTER

## 油莎豆联合收获机用脱粒清选装置设计与试验

Zixuan ZHANG<sup>1)</sup>, Honglei JIANG<sup>1)</sup>, Xiaoning HE<sup>\*1)</sup>, Fangyan ZHANG<sup>1)</sup>, Jiasheng WANG<sup>1)</sup>, Dongwei WANG<sup>1)</sup>

<sup>1)</sup>College of Electromechanical Engineering, Qingdao Agricultural University, Qingdao 266109, China;

Tel: +86-19811788356; E-mail: 19811788356@163.com

DOI: <https://doi.org/10.35633/inmateh-72-71>

**Keywords:** *Cyperus esculentus L.*, threshing and sorting devices, field testing, design

### ABSTRACT

In response to the challenges of difficult separation and incomplete cleaning during the mechanized harvesting of *Cyperus esculentus L.*, a combined threshing and cleaning device consisting of a fruit-picking roller, a cleaning belt, and an air-screening system was designed. The structure and working principle of this device were explained, and the main components and operating parameters were determined through theoretical analysis. Using fruit-picking roller speed, cleaning belt angle, and fan speed as evaluation indicators, a three-factor three-level field experiment was conducted based on the Box-Behnken central composite design principle. Regression models between loss rate, impurity rate, and significant factors were established, and the optimal working parameters were determined using regression equations. The results showed that when the fruit-picking roller speed was 543.7 r/min, the cleaning belt angle was 50.3°, and the fan speed was 532.4 r/min, the loss rate of sesame seed harvesting was 2.67%, and the impurity rate was 2.49%. The results of field validation experiments indicated that the average loss rate of the combined threshing and cleaning device under the optimal parameter combination was 2.88%, and the average impurity rate was 2.41%, which were consistent with the optimization results of the regression model and fully met the requirements of mechanized sesame seed harvesting production.

### 摘要

针对油莎豆在机械化收获过程中脱粒分离困难、清选除杂不彻底导致收获损失率、含杂率较高的难题，设计了一种摘果辊、除杂带与风筛式组合的脱粒清选装置，说明了其结构以及工作原理，通过理论分析，确定了关键零部件的主要结构以及工作参数。以摘果辊转速、除杂带倾角、风机转速为评价指标，依据 Box-Behnken 中心组合设计原理开展三水平三因素田间试验，立了损失率、含杂率与各显著因素之间的回归模型，利用回归方程解出最优工作参数，结果表明：当摘果辊转速为 543.7r/min、除杂带倾角为 50.3°、风机转速为 532.4r/min 时，油莎豆收获损失率为 2.67%，含杂率为 2.49%。田间验证试验结果表面：最优参数组合下的摘果辊与风筛式组合的脱粒清选装置平均损失率为 2.88%；平均含杂率为 2.41%，与回归模型寻优结果基本一致，完全满足油莎豆机械化收获生产需求。

### INTRODUCTION

*Cyperus esculentus L.*, also known as the tiger nut, bears fruit underground and is a metamorphic stem. (Wang et al, 2019; Sander et al, 2023). *Cyperus esculentus L.* has strong adaptability to drought and desertification, and its adventitious stem can produce high-quality oil, which is a new type of excellent oil crop for comprehensive desertification control and economic benefits. Currently, there is a large gap in the demand for edible vegetable oil production in China, with a high external dependence. Therefore, the development of the *Cyperus esculentus L.* industry is of great significance to improving China's self-sufficiency in edible oil and ensuring national food and oil security (Zhao et al, 2019; Akabassi et al, 2021; Zhang et al, 2023).

Due to the underground growth of *Cyperus esculentus L.*, the small size of the beans makes it difficult to separate from soil clumps, resulting in high mechanical harvesting loss rates and low cleanliness, severely constraining the development of the *Cyperus esculentus L.* industry (Jeroen et al, 2023).

Zixuan ZHANG, Ph.D. Stud. Eng; Honglei JIANG, Ph.D. Eng; Xiaoning HE, Ph.D. Stud. Eng; Fangyan ZHANG, Ph.D. Stud. Eng; Jiasheng WANG, Ph.D. Stud. Eng; Dongwei WANG, Ph.D. Stud. Eng

Currently, existing *Cyperus esculentus L.* harvesters often complete the processes of soil removal, threshing, and cleaning in a single step within the drum sieve, with only a few harvesters incorporating secondary threshing and cleaning devices. However, due to suboptimal structural or operational parameter configurations, there are issues with incomplete threshing and cleaning, leading to higher harvesting loss rates and impurity content (Zhang et al, 2019).

Wei Chunnai et al. designed a threshing and cleaning device for high-input rice combine harvesters, focusing on the axial flow threshing separation device and the centrifugal fan cleaning device with dual outlets, which showed good threshing and cleaning effects (Wei et al, 2018). Mao Xin et al. studied oats and threshing teeth, analyzing the effects of factors such as drum speed, feed rate, and concave screen clearance on the threshing separation performance (Mao et al, 2022). Wang Dongwei et al. designed the 4HJL2 peanut combine harvester, with a cleaning device consisting of a single duct axial flow fan and a single-layer perforated flat screen, featuring simple structure and easy installation, and exhibiting good cleaning effects on peanut seedlings and straw (Wang et al, 2013). Gao Lianxing et al. developed the 5XT-2Z peanut picker, with a cleaning device comprising an air suction fan and a vibrating screen; the vibrating screen removes small stones, soil clumps, and other impurities while uniformly conveying peanut pods, with the front suction port near the picking device removing small peanut leaves, stems, and other impurities, and the rear suction port removing floating peanut stems, empty pods, and other impurities (Gao et al, 2015).

This study addresses the issue of existing oilseed harvester machines, which often complete the threshing and sorting process in a single step within the drum sieve during harvesting, leading to difficulties in threshing and incomplete removal of impurities. A threshing and sorting device for oilseed harvesters is proposed and the structural and operational parameters of key components are determined through theoretical analysis. Based on field experiments, the optimal operating parameter combination for the threshing and sorting device is we identified and the reliability of the results obtained from the field experiments is validated.

## MATERIALS AND METHODS

### Structure design

#### ● Complete machine structure

The threshing and cleaning device is the main working component of mechanized harvesting for *Cyperus esculentus L.*, primarily responsible for separating excavated *Cyperus esculentus L.* from large amounts of soil, clumps of grass, and other impurities (Li et al, 2022). Its structural schematic is illustrated in Figure 1(a), comprising components such as the feeding conveyor belt, picking rollers, concave screens, winnowing fan, impurity removal belt, vibrating screen, and others.

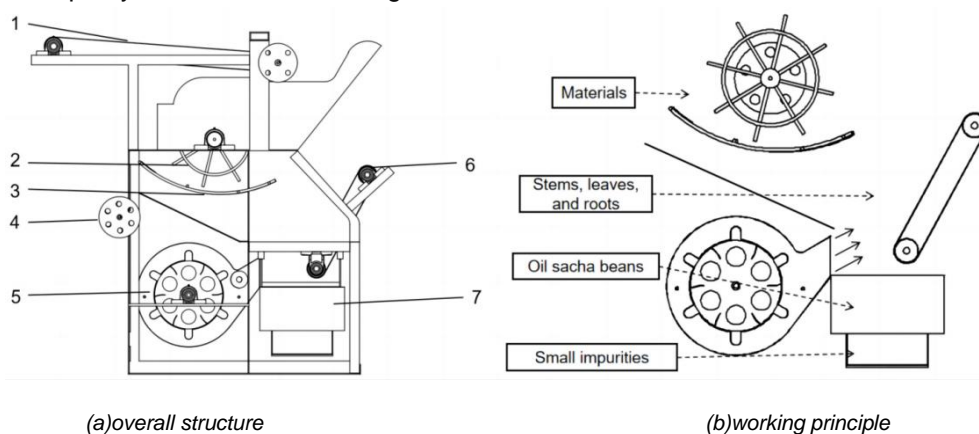


**Fig. 1 - The overall structure and working principle**

1. Feeding conveyor belt; 2. Picking rollers; 3. Concave screen; 4. Drive shaft; 5. Winnowing fan; 6. Impurity removal belt; 7. Vibrating screen

The working principle of the device is illustrated in Figure 1(b). Firstly, the feeding conveyor belt feeds the mixture of *Cyperus esculentus L.* plants and soil impurities, sieved preliminarily, into the threshing and cleaning device. Inside the chamber formed by the picking rollers and the concave screen, the material undergoes threshing and separation through the impact and rubbing actions of the threshing components.

After threshing, the material is separated into three parts: stems and leaves, soil, and beans. Stems and leaves fall into the vibrating screen below, where, under the action of the winnowing fan, the stems and leaves are blown onto the impurity removal belt and removed from the machine, while soil, short broken grass roots, and other fine impurities pass through the screen holes and fall onto the ground.

**The design of key components**

● **Design of parameters for the picking rollers**

The *Cyperus esculentus L.* plants have well-developed root systems and are prone to tillering. Several *Cyperus esculentus L.* plants often intertwine with each other, resulting in materials entering the threshing device being mostly in clumps. Therefore, it is advantageous to select threshing components with strong striking and tearing capabilities to crush clumped materials and thresh the *Cyperus esculentus L.* beans (An et al, 2022; Fu et al, 2020). In this study, a nail-shaped picking element was chosen to design the picking rollers. The collision model between the nail-shaped element and *Cyperus esculentus L.* beans is shown in Figure 2. The collision area between the spherical nail-shaped element and *Cyperus esculentus L.* beans is:

$$S = \pi[R^2 - (R - h)^2] \tag{1}$$

where:

*S* is the collision cross-sectional area, (mm<sup>2</sup>);

*R* is the radius of the spherical nail, (mm);

*h* is the collision compression amount, (mm).

Due to the strong striking and tearing capabilities of the nail-shaped element, considering the occurrence of damaged or rotten beans during the threshing process, the nail tip is specifically analyzed. The collision cross-sectional area of the spherical nail is significantly larger than that of a conventional nail. Under the same collision compression amount, the impact intensity on the beans is lower. To reduce damage to the beans by the nail, the tip of the nail is processed into a spherical shape, with a diameter of *d* = 18 mm and a length of *l* = 50 mm.

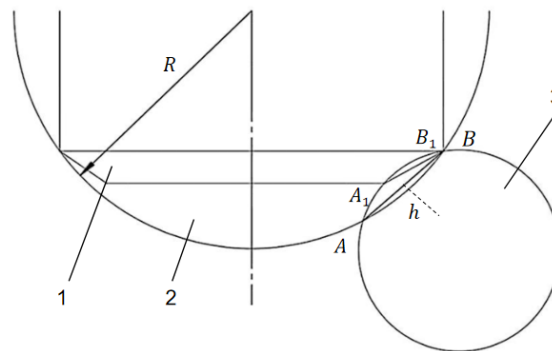


**Fig. 2 - Representation of contact between nail and bean**  
 1. Spherical nail; 2. Conventional nail; 3. *Cyperus esculentus L.* bean

The length of the threshing drum can be calculated using equation (2):

$$L = a(Z - 1) + 2\Delta l \tag{2}$$

where: *a* is the tooth pitch, (mm); *Z* is the number of threshing elements;  $\Delta l$  is the distance from the edge tooth to the end of the picking roller, (mm).

From equation (2), it can be calculated that the length of the picking roller is 960 mm. Currently, the commonly used diameter of picking rollers in combine harvesters is 450-650 mm (Ge et al, 2017), and to avoid entanglement and blockage in the material fed into the *Cyperus esculentus L.* threshing and cleaning device, the diameter of the picking roller in this study is selected as 450 mm, as shown in Figure 3.

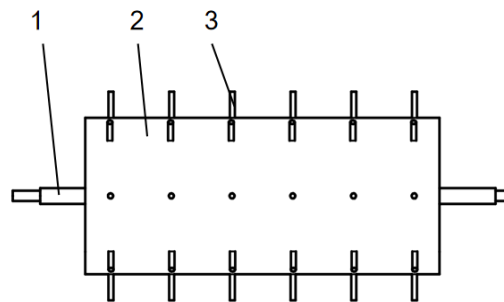


**Fig. 3 - Picking roller structure**  
 1. Picking roller drive shaft; 2. Main roller body; 3. Picking roller teeth

The threshing speed of the axial flow nail-tooth drum threshing device, which is the circumferential speed at the top of the picking roller teeth, can be initially selected as (Ji et al, 2023) 6-10 m/s due to the relatively hard texture of *Cyperus esculentus L.* beans. The relationship between the picking speed and the drum speed is given by the formula:

$$n = \frac{60v}{\pi D} \quad (3)$$

where:  $n$  is the picking roller speed, (r/min);  $D$  is the picking roller diameter, (mm).

The picking roller speed calculated from equation (3) is 347-579 r/min.

- **Design of parameters for the concave screen**

The concave screen and picking roller together form the threshing component. The concave screen mesh can comb the *Cyperus esculentus L.* beans, allowing the threshed *Cyperus esculentus L.* beans to pass through the screen under the force of gravity, while impurities such as *Cyperus esculentus L.* grass continue to move along the concave screen under the driving force of the picking roller, achieving threshing separation. Referring to existing designs and experimental results (Dong et al, 2024), square aperture grid concave screens are selected, with the concave screen aperture set at 50 mm × 50 mm and the threshing gap at 20 mm.

- **Design of parameters for the winnowing fan**

The fan is installed below the picking roller, with the outlet facing the material chute. During operation, it is powered by belt drive. Due to the force of the fan, *Cyperus esculentus L.* grass, roots, soil, and other impurities are blown onto the impurity removal belt, while the threshed *Cyperus esculentus L.* beans fall into the vibrating screen (Guo et al, 2021). The formula for calculating air volume is:

$$Q = \frac{q_0}{\mu\rho} \quad (4)$$

where:  $\rho$  is the air density, (kg/m<sup>3</sup>);  $q_0$  is the amount of impurities that the fan can clean in a unit of time, (3.6kg/s);  $\mu$  is the mixture ratio of impurity-carrying airflow, take 0.3. Substitute 0.3 into equation (4) and solve  $Q = 9.28 \text{ m}^3/\text{s}$ .

The formula for calculating blade parameters is:

$$D_2 = \frac{60\mu_2}{\pi n} \quad (5)$$

where:  $\mu_2$  is the peripheral speed of the impeller, (m/s);  $D_2$  is the impeller outer diameter, (mm);  $n$  is the fan speed, (r/min). Based on experience, it is determined 450-550 r/min.

Obtain  $D_2=450$  mm. Typically, the number of blades is chosen to be between 3 and 6 based on the layout and design of the whole machine. In this case, 6 blades are selected, as shown in Figure 4.

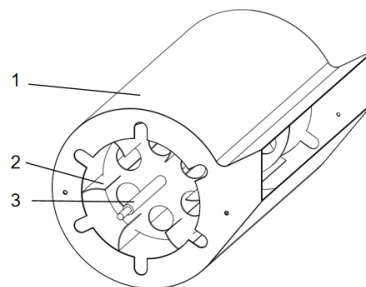


**Fig. 4 - Fan impeller structure**

1. Fan housing; 2. Fan blades; 3. Fan shaft

- **Design of the impurity removal belt**

The main function of the impurity removal belt is to eject a large number of clumps of grass from the machine, while the *Cyperus esculentus L.* beans carried in the clumps of grass are blocked by the impurity removal belt and fall back into the vibrating screen. To improve the efficiency of removing large impurities by the impurity removal belt and explore the main factors affecting the performance of the cleaning components, it is necessary to analyze the motion of the material on the impurity removal belt and conduct a dynamic analysis of the cleaning and impurity removal process. The force acting on the material on the impurity removal conveyor belt determines its motion stat, as shown in Figure 5.

The force acting on the material along the axial direction is:

$$\sum F_x = F_f + F_v - G \sin \alpha \tag{6}$$

where:

$$F_f = \mu G \sin \alpha, \quad F_v = \frac{\rho v^2 S}{2} \tag{7}$$

where:

- $\alpha$  is the angle between the impurity removal conveyor belt and the horizontal plane, (°);
- $F_f$  is the friction force between the material and the impurity removal conveyor belt, (N);
- $F_v$  is the aerodynamic thrust exerted by the airflow on the material, (N);
- $G$  is the material's own gravity, (N);
- $S$  is the frontal area of the material, (mm<sup>2</sup>);
- $\mu$  is the coefficient of friction.

$$\sum F_y = N - G \cos \alpha \tag{8}$$

where:

$N$  is the support force of the impurity removal belt on the material, (N).

From the analysis above, it is clear that the impurity removal capacity and blocking capacity of the impurity removal belt are contradictory. Referring to existing design experience (Li et al, 2024), the inclination angle of the impurity removal belt is selected 50 – 60°, and its material is chosen to be PVC grass pattern belt.

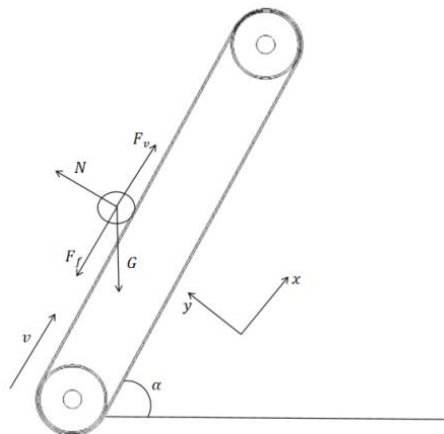


Fig. 5 - Dynamic analysis of the impurity removal process

● **Design of the vibrating screen**

The vibrating screen, together with the winnowing fan and impurity removal belt, constitutes the cleaning component. Common vibrating screens for agricultural materials include the fish scale screen, perforated screen, woven screen, and combination screen (Han et al, 2017). *Cyperus esculentus* L. beans have irregular shapes and uneven surfaces, approximately spherical, and the material entering the vibrating screen contains only a small amount of soil impurities. Therefore, it is advisable to choose a screen with good screening and separating capabilities. In this study, a flat perforated screen is selected. The width of the screen surface is related to the diameter of the picking roller, while the length of the screen surface is determined by the following formula:

$$L = \frac{Q_s}{b q_s} = \frac{Q(1-\delta K)}{b q_s} \tag{9}$$

where:

- $Q$  is the feed rate of the machine per unit time, (kg/s);
- $Q_s$  is the mass of material cleaned by the vibrating screen per unit time, (kg/s);
- $q_s$  is the feed capacity that the vibrating screen can handle, (kg/m<sup>2</sup>);
- $\delta$  is the percentage of *Cyperus esculentus* L. grass and soil in the total weight of the material;
- $k$  is the performance coefficient of the threshing and cleaning unit, typically ranging from 0.6-0.9;
- $b$  is the width of the screen surface, (m).

According to Equation (9), there is  $L=80$  cm. Considering the layout and design of the whole machine (Yu et al, 2020; Wang et al, 2022; Hou et al, 2019), the length of the swinging rod is taken as 150 mm, the diameter of the eccentric wheel is 160 mm, and the eccentric radius of the eccentric wheel is 20 mm. When the crank swinging rod is in the horizontal position, the maximum amplitude of the vibrating screen is 30 mm, and the crank speed is 250 r/min. Square sieve holes are used, with a diameter of 9 mm x 9 mm.

### ● Field experiments

Prototype construction of the threshing and cleaning unit for the *Cyperus esculentus L.* bean combined harvester will be conducted. Based on the previous determinations of parameters such as the rotation speed of the picking roller, fan speed, and inclination angle of the cleaning belt, field experiments will be carried out. Through orthogonal regression analysis, the optimal combination of working parameters will be determined.

### ● Experimental Materials

The experimental prototype used in the experiment is a 4YQL-1500 trailed oil *Cyperus esculentus L.* combined harvester, whose overall structure is shown in Figure 6. The oil *Cyperus esculentus L.* combined harvester prototype consists of several key components, including the chassis, digging device, lifting and soil removal device, cylinder screen, walking device, and threshing and cleaning device. The prototype is powered by a tractor. The digging device adopts an adjustable dual oil cylinder structure, facilitating the adjustment of digging depth. The lifting and soil removal device is designed as a flat screen structure, directly connected to the digging device, capable of preliminarily removing large chunks of soil from the oil *Cyperus esculentus L.* plants and soil and conveying them into the cylinder screen. The cylinder screen is of a single-layer design, separating most of the soil through rotation, and then conveying the soil-removed oil *Cyperus esculentus L.* plants to the threshing and cleaning device via a conveyor belt.

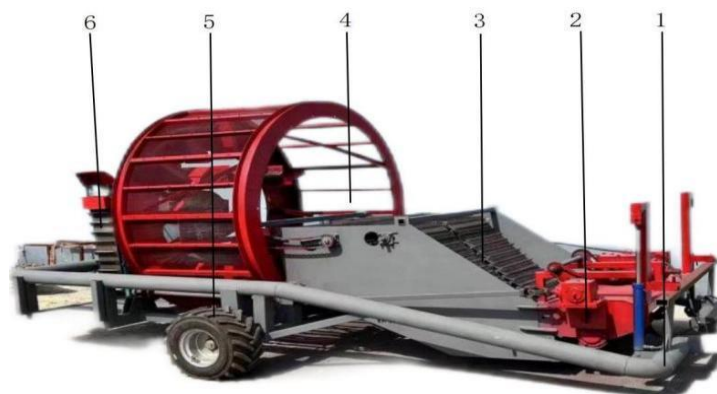


**Fig. 6 - 4YQL-1500 *Cyperus esculentus L.* Joint Harvester**

1. Chassis; 2. Digging device; 3. Lifting and soil removal device; 4. Cylinder screen; 5. Walking device; 6. Threshing and cleaning device

The experiment was conducted from October 7, 2023, to November 13, 2023, using a homemade 4YQL-1500 *Cyperus esculentus L.* Joint Harvester prototype at the Oil Sorghum Planting Demonstration Base in Minquan County, Henan Province. The oil sorghum used in the experiment was obtained from the Oil Sorghum Planting Demonstration Base in Minquan County, Henan Province, and the variety was "Yu Oil Sorghum No.5". Experimental instruments included the JM-B1003 electronic counting balance, TSC electronic scale, CASIO calculator, vernier caliper, protractor, etc.

### ● Experimental Method

The experiment was conducted following the methods specified in GBT 5262-2008 "General Rules for Determination Methods of Test Conditions for Agricultural Machinery", GB/T 5667 "Test Methods for Agricultural Machinery Production", and GBT25235-2010 "Combined Cleaning Sieve for Grain and Oil Machinery". Loss rate determination: Upon completion of the operation of the *Cyperus esculentus L.* harvester, impurities were collected after cleaning, and *Cyperus esculentus L.* grains were manually sorted out and weighed. Measurement of harvested *Cyperus esculentus L.* mass: After completion of the operation of the sample machine, the total weight of the *Cyperus esculentus L.* in the collection box was measured. Impurity content determination: After the sample machine completed harvesting, the collection box was overturned, and the *Cyperus esculentus L.* grains were poured out. Impurities were manually picked out and weighed. Loss rate and impurity content calculation are illustrated in Figures 7 and 8, respectively, and are calculated using formulas (10) and (11) as shown below.



Fig. 7 - Loss rate measurement



Fig. 8 - Impurity rate weighing

$$L_1 = \frac{Q_4}{Q_1+Q_3+Q_4} \times 100\% \tag{10}$$

$$L_2 = \frac{Q_1}{Q_1+Q_3} \times 100\% \tag{11}$$

where:

$L_1$  is the loss rate, (%);  $L_2$  is the Impurity rate, (%);  $Q_1$  is the mass of impurities carried with beans, (kg);  $Q_3$  is the harvested bean mass, (kg);  $Q_4$  is the impurity mass, (kg).

This experiment utilized Design-Expert 8.0.6 software for experimental design. The Box-Behnken response surface methodology with a 3-factor, 3-level design was employed. The factors chosen were the rotational speed of the fruit-picking roller (A), the inclination angle of the debris-removing belt (B), and the rotational speed of the fan (C). Loss rate ( $Y_1$ ) and impurity rate ( $Y_2$ ) were selected as evaluation indices.

The ranges of the selected factor levels were as follows: fruit-picking roller speed ranging from 350 to 550 rpm, debris-removing belt inclination angle ranging from 50 to 60 degrees, and fan speed ranging from 450 to 550 rpm. The factors were coded as 1, 0, and -1, respectively, and the experimental codes are detailed in Table 1.

Table 1

Factor level coding table

Levels	Factors		
	Harvester roller speed (r/min)	Angle of the debris belt (°)	Blower speed (r/min)
1	350	50	450
0	450	55	500
-1	550	60	550

Table 2

Test scheme and results

Experiment Number	Factors			Experiment Results	
	A	B	C	Y1 (%)	Y2 (%)
1	350	50	500	4.66	2.50
2	550	50	500	5.60	2.56
3	350	60	500	3.46	1.64
4	550	60	500	3.98	2.97
5	350	55	450	5.10	1.09
6	550	55	450	4.22	2.83
7	350	55	550	1.90	2.03
8	550	55	550	5.10	1.74
9	450	50	450	3.28	2.82
10	450	60	450	5.16	1.07
11	450	50	550	5.10	1.05

**Table 2**  
(continuation)

Test scheme and results					
Experiment Number	Factors			Experiment Results	
	A	B	C	Y1 (%)	Y2 (%)
12	450	60	550	1.54	2.43
13	450	55	500	2.22	2.31
14	450	55	500	2.32	1.92
15	450	55	500	3.10	1.83
16	450	55	500	2.26	1.98
17	450	55	500	2.22	2.06

● **Establishment of the regression equation and variance analysis**

For the regression model of loss rate, factors A, B, C, BC, B<sup>2</sup>, and AC have extremely significant effects on the loss rate (P < 0.01), while the interaction term C<sup>2</sup> has a significant effect on the loss rate (P < 0.05). Judging by the F-values, the primary and secondary order of significance of the first-order terms on the loss rate are B, C, and A, respectively.

For the regression model of impurity rate, factors A, AB, AC, BC, and C<sup>2</sup> have extremely significant effects on the impurity rate (P < 0.01), and factor A<sup>2</sup> has a significant effect on the impurity rate (P < 0.05). Based on the F-values, the primary and secondary order of significance of the first-order terms on the impurity rate are A, B, and C, respectively.

**Table 3**

ANOVA for loss rate and impurity rate				
Sources of Variance	Loss rate		Impurity rate	
	F	P	F	P
Model	345.43	<0.0001	102.48	<0.0001
A	14.43	0.0067	49.32	0.0002
B	20.45	0.0027	4.11	0.0822
C	17.14	0.0043	1.92	0.2087
AB	0.36	0.5694	19.72	0.0030
AC	33.61	0.0007	50.40	0.0002
BC	59.76	<0.0001	119.81	<0.0001
A <sup>2</sup>	45.41	0.0003	11.74	0.0110
B <sup>2</sup>	24.31	0.0017	5.19	0.0568
C <sup>2</sup>	8.52	0.0224	23.29	0.0019
Lack of fit term	0.67	0.3237	0.097	0.9577

Using Design-Expert software, multiple regression fitting analysis was conducted. After eliminating the non-significant factors, regression equations were established separately for loss rate and impurity rate with significant factors.

$$Y_1 = 2.42 + 0.47A - 0.56B - 0.52C - 0.11AB + 1.02AC - 1.36BC + 1.16A^2 + 0.85B^2 + 0.50C^2 \tag{12}$$

$$Y_2 = 2.02 + 0.36A - 0.10B - 0.07C + 0.32AB - 0.51AC + 0.78BC + 0.24A^2 + 0.16B^2 - 0.34 \tag{13}$$

From Table 3, it can be observed that the regression models for separation rate and impurity rate are both highly significant (P < 0.01), while the lack of fit terms are not significant (P > 0.05). This indicates that the fitted regression equations are highly reliable. Therefore, optimal parameter combinations for the three factors can be determined based on the aforementioned regression models.

● Analysis of the impact of interaction effects on experimental indicators

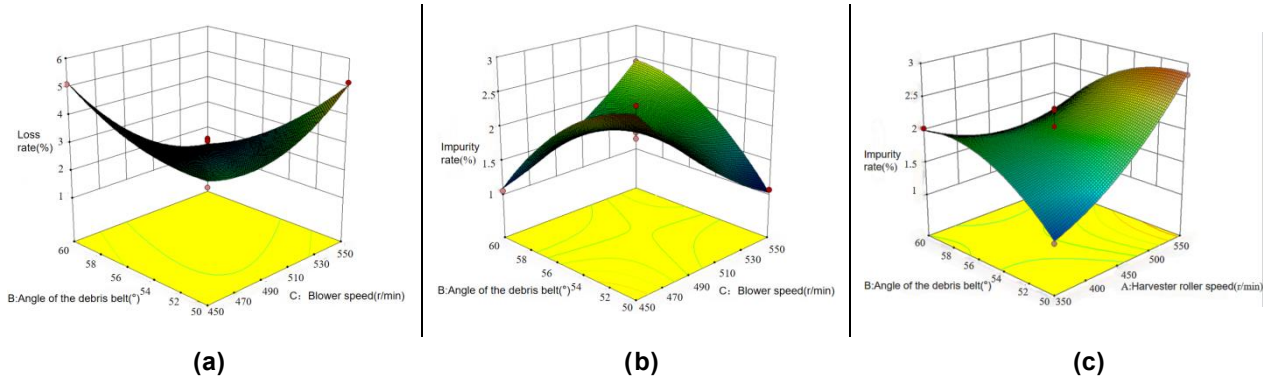


Fig. 9 - Response surfaces for effect of factors interaction on test indicators

The response surface of the impact of the interaction effects on the loss rate and impurity content rate was obtained through Design-Expert software, as shown in Figure 9. In Figure 10a, the contour curvature is larger compared to Figure 10b, indicating that the interaction between the inclination angle of the impurity removal belt and the fan speed has a more significant effect on the impurity content rate compared to the interaction between the inclination angle of the impurity removal belt and the roller speed. From Figure 10c, it can be observed that the loss rate is positively correlated with the fan speed and negatively correlated with the inclination angle of the impurity removal belt. The inclination angle of the impurity removal belt has a more significant impact on the response surface because as the inclination angle of the impurity removal belt increases, it can create a blocking effect on the separated *Cyperus esculentus L.* during the falling process under the action of the blowing fan airflow, leading to a rapid decrease in the loss rate.

● Solving for the optimal combination of experimental factors

Based on the above experimental results and regression equations, with the optimization objectives being to minimize loss rate and impurity rate, and with the optimization variables being fruit picking roller speed, inclination angle of the impurity removal belt, and fan speed, the regression model is optimized. The objective function and constraints are as follows:

$$\begin{cases} \min Y_1(A, B, C) \\ \min Y_2(A, B, C) \\ \text{s. t. } \begin{cases} 350 \leq A \leq 550 \\ 50 \leq B \leq 60 \\ 450 \leq C \leq 550 \end{cases} \end{cases} \quad (14)$$

The optimal operating parameters for the threshing and cleaning device are determined to be: fruit picking roller speed of 543.7 r/min, inclination angle of the impurity removal belt of 50.3°, and fan speed of 532.4 r/min. With these settings, the operational performance is optimized. Theoretical performance indicators for the optimized threshing and cleaning device are as follows: loss rate ( $Y_1$ ) is 2.67%, and impurity rate ( $Y_2$ ) is 2.49%.

● Validation experiment

Based on Table 4, the average loss rate of the traction-type oil *Cyperus esculentus L.* combined harvester's threshing and cleaning device under the optimal parameter combination obtained from the field validation experiment is 2.88%, and the average impurity rate is 2.41%, which is consistent with the results of the regression model optimization.

The machine operates smoothly during the entire operation, with outstanding threshing and cleaning effects, fully meeting the requirements for oil sunflower harvesting work. The validation experiment is depicted in Figure 10.

Table 4

Validation test results

Trial number	Loss rate	Impurity rate
1	3.03%	2.32%
2	2.57%	2.47%
3	2.65%	2.09%
4	3.28%	2.74%
Mean value	2.88%	2.41%



Fig. 10 - Verification test

## CONCLUSIONS

(1) A threshing and cleaning device for a *Cyperus esculentus L.* combine harvester was designed aiming to address the challenges of completing the threshing and cleaning process within the drum sieve, leading to difficulties in threshing separation and inadequate cleaning of impurities. Through theoretical analysis, the structural and operational parameters of key components were determined.

(2) Based on the Box-Behnken experimental design principle, a field experiment with three factors and three levels was conducted using the fruit picking roller speed, the angle of the debris removal belt, and the fan speed as influencing factors, while the loss rate and impurity rate were used as evaluation indicators. The results indicate that when the fruit picking roller speed is 543.7 r/min, the angle of the debris removal belt is 50.3°, and the fan speed is 532.4 r/min, the loss rate of harvested *Cyperus esculentus L.* is 2.67%, and the impurity rate is 2.49%.

(3) Field validation experiment results show that the average loss rate of the combined fruit picking roller and wind sieve type separation and cleaning device under the optimal parameter combination is 2.88%, and the average impurity rate is 2.41%. These results are consistent with the optimization results of the regression model, fully meeting the requirements of mechanized harvesting production for *Cyperus esculentus L.*

## ACKNOWLEDGEMENT

This work has been supported by Henan Provincial Major Science and Technology Project (Project No.211100110100); Youth Project of Natural Science Foundation of Shandong Province (Project No.ZR2022QE167); Shandong Province Technology Innovation Guidance Programme (Project No.YDZX2023005)

## REFERENCES

- [1] Akabassi G.C., Palanga K.K., Padonou E.A. (2021) A Global Systematic Review on Biology, *Production Constraints and Uses of Cyperus exculentus L.* Preprints, Vol.2, pp.42-44, United States.
- [2] An S. (2022). Design and test of the separation device (油莎豆脱粒分离装置的设计与试验). *Master's degree (dissertation, Shihezi University)*. Xinjiang/China.
- [3] Dong R., Xiao J., Liu W., Guo W., Wang X., Liu F. (2024). Design and test of traction oil harvester (牵引式油莎豆收获机设计与试验). *China Agricultural Machinery Chemical News*. Vol.1, pp.21-27. Jiangsu/China.
- [4] Fu J., Zhang Y., Cheng C., Chen Z., Tang X., Ren L. (2020). Design and test of rigid and flexible coupling of wheat (刚柔耦合式小麦脱粒弓齿设计及试验). *Journal of Jilin University (Engineering Edition)*. Vol. 2, pp. 730-738. Jilin/China.
- [5] Gao L., Li X., Guan M. (2015) Design and test of peanut fruit cleaning device with double suction outlet (双吸风口振动式花生荚果清选装置设计与试验). *Journal of Agricultural Machinery*, Vol. 46, pp. 110-117. Beijing/China.
- [6] Ge Q. (2017). Design and study of key technology of longitudinal axial flow threshing drum device of combine harvester (联合收割机纵轴流脱粒滚筒装置关键技术设计与研究). *Heilongjiang Science and Technology Information*. Vol. 8, pp. 80-81. Heilongjiang/China.
- [7] Guo P., Shang S., Wang D., He X., Xu N., Liu J., Dong M. (2021). Design and test of traction-type peanut picking harvester (牵引式花生捡拾收获机的设计与试验). *Agricultural mechanization research*. Vol. 12, pp. 92-97. Heilongjiang/China.

- [8] Han C., Liu X., Zhang X. (2017). Design and experimental study of oil sunflower and of oil plant (油葵脱粒清选装置的设计与试验研究). *Journal of Xinjiang Agricultural University*. Vol.6 pp.454-459. Xinjiang/China.
- [9] Hou J., Ren Z., Zhu H. (2022). Design and test of double-layer inclined vibration air screen castor cleaning device (双层倾斜振动风筛式蓖麻清选装置设计与试验). *Journal of Agricultural Machinery*. Vol.S2. pp. 39-51. Beijing/China.
- [10] Ji M. (2023). Design and experimental study of threshing device (横轴流油莎豆脱粒装置的设计与试验研究). *Master's degree (dissertation, Jilin Agricultural University)*. Jilin/China.
- [11] Jeroen Feys, Dirk Reheul, Wolf De Smet, Shana Clercx, Sander Palmans, Gert Van de Ven & Benny De Cauwer. (2023). Effect of anaerobic soil disinfestation on tuber vitality of yellow nutsedge (*Cyperus esculentus*). *Agriculture* (8).
- [12] Li J., Liu W., Zhang L. (2022). Design and testing of oil and *Cyperus esculentus* L. harvest equipment (油莎豆收获装备设计与试验). *Agricultural Engineering*, Vol. 4, pp. 36-39. Beijing/China.
- [13] Li D., Wang D., He X., Zuo B., Zhang C., Li X. (2024). Study on the secondary clearance of peanut semi-feeding and combined harvest (花生半喂入联合收获二次清选机构研究). *China Agricultural Machinery Chemistry*. Vol. 3, pp.117-125. Jiangsu/China.
- [14] Mao X., Zhao R., Yi S. (2022). Experimental study of secondary orthogonal rotation combination of naked oat threshing and separation device (裸燕麦脱粒与分离装置二次正交旋转组合试验研究). *Agricultural mechanization research*, Vol. 9, pp. 181-188. Beijing/China.
- [15] Sander De Ryck, Dirk Reheul & Benny De Cauwer. (2023). Impact of regular mowing, mowing height, and grass competition on tuber number and tuber size of yellow nutsedge clonal populations (*Cyperus esculentus* L.). *Weed Research*. Vol. 6, pp. 371-381. United Kingdom.
- [16] Wang R., Wang X., Xiang H. (2019). A versatile emerging oil crop (一种多用途的新兴油料作物). *Chinese fats*, Vol. 1, pp. 1-4, Shanxi/China.
- [17] Wei C., Li Y., Xu L. (2018). Design and testing of feeding rice combine harvester (大喂入量水稻联合收获机脱粒清选装置的设计与试验). *Agricultural mechanization research*, Vol.8, pp.5, Heilongjiang/China.
- [18] Wang D. (2013). Research on key device of peanut joint harvester (花生联合收获机关键装置的研究), *PhD (dissertation, Shenyang Agricultural University)*. PhD. Thesis. Liaoning/China.
- [19] Wang L., Liu W., Li Y., Yu K. (2022). Study on shaking plate of clearing system of corn grain harvester (大喂入量玉米籽粒收获机清选系统双层筛孔抖动板研究). *Journal of Agricultural Machinery*. Vol.7 pp.92-102. Beijing/China.
- [20] Yu X. (2020). Design and experimental study of small peanut fruit picker (小型花生摘果机的设计与试验研究). *Master's degree (dissertation, Xinjiang Agricultural University)*. Xinjiang/China.
- [21] Zhao Y., Zou X., Zhang Y., Han Z., Zeng L., Zhang X. (2019). *Cyperus esculentus* L. High oil and high yielding variety *Cyperus esculentus* L. 1, China (油莎豆高油高产品种中油莎 1 号). *China seed industry*, Vol. 6, pp. 96-97, Beijing/China.
- [22] Zhang S., Zhang R., Cao Q. (2023). Design and test of double-layer roller sieve fruit mixed separation device for oil *Cyperus esculentus* L. harvester (油莎豆收获机双层滚筒筛式果杂分离装置设计与试验). *Journal of Agricultural Machinery*, Vol. 54, pp. 148-157, Beijing/China.
- [23] Zhang B., Liu J., Fan Z. (2019). Research progress on mechanized sowing and harvesting technology and equipment of saline-alkali earth oil and bean (盐碱地油莎豆机械化播种收获技术与装备研究进展). *Shandong Agricultural Science*, Vol. 51, pp. 4, Shandong/China.